

Involvement of GABAergic and Cholinergic Medial Septal Neurons in Hippocampal Theta Rhythm

Ryan M. Yoder and Kevin C.H. Pang*

ABSTRACT: Hippocampal theta rhythm (HPC θ) may be important for various phenomena, including attention and acquisition of sensory information. Two types of HPC θ (types I and II) exist based on pharmacological, behavioral, and electrophysiological characteristics. Both types occur during locomotion, whereas only type II (atropine-sensitive) is present under urethane anesthesia. The circuit of HPC θ synchronization includes the medial septum-diagonal band of Broca (MSDB), with cholinergic and γ -aminobutyric acid (GABA)ergic neurons comprising the two main projections from MSDB to HPC. The primary aim of the present study was to assess the effects of GABAergic MSDB lesions on urethane- and locomotion-related HPC θ , and compare these effects to those of cholinergic MSDB lesions. Saline, kainic acid (KA), or 192 IgG-saporin (SAP) was injected into MSDB before recording. KA preferentially destroys GABAergic MSDB neurons, whereas SAP selectively eliminates cholinergic MSDB neurons. A fixed recording electrode was placed in the dentate mid-molecular layer, and stimulating electrodes were placed in the posterior hypothalamus (PH), and medial perforant path (PP). Under urethane anesthesia, HPC θ was induced by tail pinch, PH stimulation, and systemic physostigmine; none of the rats with KA or SAP showed HPC θ in any of these conditions. During locomotion, HPC θ was attenuated, but not eliminated, in rats with KA or SAP lesions. Intraseptal KA in combination with either intraseptal SAP or PP lesions reduced locomotion-related HPC θ beyond that observed with each lesion alone, virtually eliminating HPC θ . In contrast, intraseptal SAP combined with PP lesions did not reduce HPC θ beyond the effect of each lesion alone. We conclude that both GABAergic and cholinergic MSDB neurons are necessary for HPC θ under urethane, and that each of these septohippocampal projections contributes to HPC θ during locomotion. © 2005 Wiley-Liss, Inc.

KEY WORDS: septum; GABA; acetylcholine; hippocampus; entorhinal

INTRODUCTION

Hippocampal recordings reveal a prominent 4–10-Hz field potential oscillation, known as theta rhythm (HPC θ) (Green and Arduini, 1954). Hippocampal theta rhythm is prominent during urethane anesthesia, voluntary movement, and paradoxical sleep, but not during “automatic” activities such as grooming and chewing (Vanderwolf, 1969). Two types of HPC θ have been distinguished on the basis of pharmacological sensitivity, frequency, and behavior (Vanderwolf, 1975; Kramis et al., 1975; Montoya and Sainsbury, 1985). Type II HPC θ (HPC θ -2), but not type I HPC θ (HPC θ -1), is eliminated by muscarinic receptor antagonists such as atro-

pine. Peak frequency of HPC θ -1 is 6–10 Hz, whereas HPC θ -2 has a lower frequency peak, usually 4–6 Hz. Finally, HPC θ -1 and HPC θ -2 co-occur during locomotion, whereas only HPC θ -2 occurs during immobility and urethane anesthesia.

The medial septum/diagonal band of Broca (MSDB) is a critical component of the ascending circuit responsible for HPC θ synchronization (Green and Arduini, 1954). Electrolytic lesion or inactivation of MSDB with tetracaine or procaine interrupts rhythmic hippocampal unit activity, reduces motor activity (Mizumori et al., 1989; Oddie et al., 1996), and eliminates HPC θ (Green and Arduini, 1954; Winson, 1978; Givens and Olton, 1990; Lawson and Bland, 1993; Partlo and Sainsbury, 1996). The major septal neurons projecting to the hippocampus use acetylcholine (ACh) or γ -aminobutyric acid (GABA) as neurotransmitters (Freund, 1989; Kiss et al., 1997). These neurons send their axons to the hippocampus through the fimbria-fornix which, when transected, result in a loss of HPC θ (M'Harzi and Monmaur, 1985).

Several types of MSDB neurons have activity that is phase-locked to HPC θ and have been distinguished on the basis of action potential waveform (Brazhnik and Fox, 1997). Medial septal neurons with a brief-spike and brief-afterhyperpolarization (AHP) were resistant to acetylcholine (ACh) antagonists and were tentatively classified as GABAergic. Rhythmically firing, long-spike, long-AHP cells were sensitive to ACh antagonists and were proposed to be cholinergic neurons. These results suggest that ACh antagonists (i.e., atropine) eliminate HPC θ by inhibiting MSDB cholinergic cells. In support of this idea is the finding that intraseptal infusion of atropine eliminates HPC θ -2 (Monmaur and Breton, 1990; Lawson and Bland, 1993). However, a recent study found that ACh predominantly excites noncholinergic but not cholinergic MSDB neurons (Wu et al., 2000), suggesting that intraseptal atropine eliminates HPC θ by acting directly on noncholinergic MSDB neurons. Therefore, it is still unclear what roles cholinergic and GABAergic MSDB neurons have in the synchronization of HPC θ .

Cholinergic MSDB lesions made by 192 IgG-saporin (SAP) injection reduce the amplitude, but do not eliminate HPC θ during locomotion (Lee et al., 1994). As mentioned earlier, HPC θ during locomotion may consist of two types. Albeit reduced, the presence of HPC θ after cholinergic MSDB lesions suggests that GABAergic

Department of Psychology, J.P. Scott Center for Neuroscience, Mind and Behavior, Bowling Green State University, Bowling Green, Ohio

Grant sponsor: U.S. Public Health Service (USPHS); Grant number: NS044373; Grant sponsor: Dorothy Price.

*Correspondence to: Kevin C.H. Pang, J.P. Scott Center for Neuroscience, Mind and Behavior, Department of Psychology, Bowling Green State University, Bowling Green, OH 43403. E-mail: kpang@bgnet.bgsu.edu

Accepted for publication 18 October 2004

DOI 10.1002/hipo.20062

Published online in Wiley InterScience (www.interscience.wiley.com).

and cholinergic MSDB neurons are responsible for distinct components of the locomotion-related HPC θ activity (Heynen and Bilkey, 1991; Vanderwolf, 1975). Alternatively, GABAergic MSDB neurons may be primarily responsible for pacing the synchronization of HPC θ with cholinergic neurons having the supporting role of amplifying the synchronization (Lee et al., 1994; Stewart and Fox, 1990). Supporting both ideas, lesions of MSDB cholinergic and GABAergic cells eliminate HPC θ during locomotion (Gerashchenko et al., 2001). One way to determine the roles of MSDB cholinergic and GABAergic involvement in hippocampal function is to determine whether a selective lesion of septal GABAergic neurons is sufficient to eliminate HPC θ . To date, these studies have not been conducted because of the difficulty in producing selective lesions of MSDB GABAergic neurons.

Intraseptal administration of some excitotoxins preferentially damage noncholinergic basal forebrain neurons (Dunnett et al., 1991). In the MSDB, low doses of kainic acid (KA) or ibotenic acid destroy GABAergic neurons, while sparing most cholinergic cells (Malthe-Sørensen et al., 1980; Cahill and Baxter, 2001; Pang et al., 2001). Recently, these treatments have been used to assess the importance of MSDB GABAergic neurons in spatial memory (Cahill and Baxter, 2001; Pang et al., 2001). In the present study, we compared the effects of KA lesions of MSDB GABAergic neurons and SAP lesions of MSDB cholinergic neurons on HPC θ during urethane anesthesia and locomotion. We also examined the interaction effects of selective MSDB lesions and damage to the projection from entorhinal cortex on HPC θ .

MATERIALS AND METHODS

Subjects

Female Sprague-Dawley ($n = 4$; 225–300 g) and male Long-Evans ($n = 35$; 300–450 g) adult rats were used in the study. Rats were single-housed in a colony room with a 12-h light/dark cycle. All recordings occurred during the light phase. Most rats had been used previously for behavioral testing. All procedures involving animal housing and treatment followed National Institute of Health (NIH) guidelines and were approved by the Bowling Green State University Animal Care and Use Committee.

Surgery

Neurotoxin injection

Rats received intraseptal injection of saline, KA, or SAP at least 2 weeks before electrophysiological recording or electrode implantation. Rats were anesthetized with sodium secobarbital (50 mg/kg, i.p., supplemented as necessary) before surgery. Scopolamine methyl bromide (0.02 mg/kg, i.p.) was administered to reduce secretions. Body temperature was maintained at 37°C with a Delta-phase isothermal pad (Braintree Scientific, Braintree, MA). Each animal was placed in a stereotaxic apparatus with bregma and lambda on the same horizontal plane. Holes were drilled in the skull over MSDB. A Hamilton syringe (Hamilton Company, Reno, NV) was inserted into the medial septum (bregma +0.6

mm anteroposterior [AP], –1.5 mm mediolateral [ML], –6.3 mm dorsoventral [DV], 15° toward midline) and 0.5 μ l saline (0.9% NaCl), KA (1.0 μ g/ μ l), or SAP (0.25 μ g/ μ l) was injected at 0.1 μ l/min. An additional injection of 0.4 μ l was administered to each horizontal limb of the diagonal band of Broca at the same rate (bregma +0.6 mm AP, \pm 0.7 mm ML, –7.8 mm DV). After each injection, the drug was allowed to diffuse 5 min before removal of the syringe needle.

Electrode implantation

To record from unanesthetized rats, electrodes were implanted in control ($n = 7$), KA-treated ($n = 7$), and SAP-treated ($n = 11$) rats. Preparation for surgery was the same as for toxin injections. Holes were drilled over the posterior hypothalamus (PH), HPC, and medial perforant path (PP) for placement of stimulating or recording electrodes. A recording electrode constructed from Teflon-insulated 75- μ m stainless steel wire (A-M Systems, Everett, WA) was lowered into the dentate middle molecular layer (bregma –4.0 mm AP, –2.5 mm ML, DV determined by maximum field excitatory postsynaptic potential (fEPSP) negativity in response to medial PP stimulation). Although recording near the hippocampal fissure provides the greatest amplitude HPC θ the middle molecular layer was chosen as the recording site because it could be located accurately and reproducibly in all rats, including those with no HPC θ . Monopolar stimulation electrodes constructed of Teflon-insulated 125- μ m stainless steel wire (insulation removed 500 μ m from the tip) were placed with the electrode tip in PH (bregma –3.5 mm AP, –0.5 mm ML, –6.8 mm DV) and medial PP (bregma –7.5 mm AP, –3.8 mm ML, DV determined by maximum population spike recorded in dentate hilus in response to PP stimulation). Two Teflon-insulated 250- μ m stainless steel wires were placed in the frontal cortex; one served as a recording indifferent and the other served as a stimulating indifferent electrode. Electrodes were cemented with dental acrylic to eight stainless steel screws positioned in the frontal, parietal, and occipital bones. Electrode and indifferent leads were inserted into a Centi-loc connector (ITT Cannon; Santa Ana, CA).

Recording

Electrode leads were connected to a headstage containing a noninverting operational amplifier (1 \times) with junction field effect transistor (JFET) inputs configured as a voltage source follower. Electrical signals were amplified (\times 1,000) and filtered. A 1–10,000 Hz bandpass filter was used for fEPSP responses, and a 1–150-Hz (anesthetized recordings) or 1–40-Hz (unanesthetized recordings) bandpass filter was used for electroencephalogram (EEG) signals. Differences in bandpass filters for anesthetized and unanesthetized recordings did not affect power and amplitude measures of HPC θ (4–12 Hz). The amplified signal was monitored on a digital oscilloscope (Tektronix; Beaverton, OR) and saved on an IBM 486 computer with Experimenter's Workbench software (Datawave Technologies, Longmont, CO) at a sampling rate of 512 Hz. Electrical stimulation was delivered by constant-current stimulus isola-

tion units (SC-100; Winston Electronics, Milbrae, CA) controlled by a timer (A-65; Winston Electronics).

Anesthetized recording-depth profile

To determine the effects of intraseptal KA on HPC θ throughout the HPC, a depth profile of HPC θ (power at peak frequency) was constructed. EEG records were obtained from recording sites between the dentate hilus and CA1 pyramidal cell layer; each site was separated by 100 μ m. Control ($n = 2$) and KA-treated ($n = 2$) rats were anesthetized with urethane (1.3g/kg, i.p.) and placed in a stereotaxic apparatus. Teflon-insulated stainless steel electrodes were inserted into the PH, HPC, and PP as described for electrode implantation. Two records were obtained at each recording site. The first record consisted of an fEPSP induced by cathodal PP stimulation (200 μ A, 200 μ s) to enable determination of the HPC layer, a 15-s baseline EEG, a 10-s tail pinch-induced EEG, and a 35-s poststimulus EEG. The second record consisted of a 15-s baseline EEG, a 10-s electrical PH stimulus-induced EEG (400- μ A, 100-Hz, 100- μ s pulse duration), and a 35-s poststimulus EEG. After recording, electrode locations were marked by administering a 20-s pulse of anodal current at 50 μ A.

Anesthetized recording: middle molecular layer

Rats were anesthetized with urethane and placed in a stereotaxic apparatus, as described for depth profile recordings. Some rats (control $n = 3$; KA $n = 3$; SAP $n = 4$) were used in both anesthetized and unanesthetized recordings; for these rats, anesthetized recordings occurred at least 1 day after unanesthetized recording. EEG was recorded during baseline, tail-pinch stimulation, PH stimulation, and poststimulus periods. Three trials were administered with tail pinch, and three trials with PH stimulation as described for depth profile. At the end of the baseline and stimulation recording sessions, rats were injected with physostigmine sulfate (1.0 mg/kg body weight, i.p.); 1-min EEG episodes were recorded without PH or tail pinch stimulation beginning at 5, 10, 15, 20, 25, and 30 min post-injection.

Unanesthetized recording

After electrode implantation, rats were handled daily before recording, and were habituated to the headstage and cable. At the beginning of the recording session, rats showed no signs of elevated anxiety and navigated freely about the table. EEG records (from fixed electrodes located in the dentate middle molecular layer) were acquired in 1-s periods for 5 min. During the recording sessions, a researcher monitored the rats via video surveillance and coded the records for transitions between locomotion and immobility. After the recording session, some control, KA-treated, and SAP-treated rats received bilateral PP lesions (1.0-mA cathodal current, 1 min) 1 day before a second unanesthetized recording session.

Data Analysis

Anesthetized recordings

Hippocampal EEG records were analyzed offline with Fast Fourier Transform (FFT). FFT analysis of EEG provided power (mV^2)

at each frequency within 2–15 Hz (i.e., integrated power at 3.5–4.49 Hz was designated the power at 4 Hz). None of the rats under urethane anesthesia demonstrated a peak in the power spectrum (peak frequency) that was <4 Hz or >9 Hz. Amplitude at peak frequency was calculated as the square root of the power at peak frequency. Amplitude values were then divided by 1,000 to compensate for the $1,000\times$ gain of the recording amplifier. Peak frequency and amplitude at peak frequency were compared between control, KA-treated, and SAP-treated rats for each stimulus condition (tail pinch, PH, physostigmine). Integrated amplitude at 12–15 Hz was calculated to determine whether frequencies outside the HPC θ range were altered by the lesions. Analysis of variance (ANOVA) and Scheffé's post hoc analysis were used to compare peak frequency and amplitude at peak frequency between treatment groups.

For the depth profile, the EEG was recorded at 100- μ m intervals between the dentate hilus and CA1. FFT analysis of EEG provided integrated power at 5–8 Hz (range of observed frequency peaks in these rats) at each recording location. Depth profiles were constructed for saline- and KA-treated rats. Data from the mid-molecular layer obtained during depth profile recordings were included in the overall analysis.

Unanesthetized recordings

Hippocampal EEG records included 5 min of 1-s periods. Periods immediately before and after transition labels (between locomotion and immobility) were not analyzed. Because peak frequency during locomotion is higher than during urethane anesthesia, power at each frequency within 6–10 Hz (range of frequency peaks observed during locomotion) and integrated power at 12–15 Hz were computed by FFT analysis, from which the square root was calculated to provide the amplitude at peak frequency and integrated amplitude at 12–15 Hz. ANOVA and Scheffé's post hoc comparisons were used to compare peak frequency, amplitude at peak frequency, and integrated amplitude at 12–15 Hz between control, KA-treated, and SAP-treated rats.

Our main analysis using FFT on 1-s recording epochs had an effective resolution of 1 Hz. Because alterations in peak frequency produced by MSDB treatments may be subtle and <1 Hz, a second analysis with greater resolution was used. Lomb's analysis was conducted on continuous EEG records of ≥ 3 s from control, KA, and SAP rats. The advantage of Lomb's analysis is that the resolution is not limited by the length of the sample (Manis et al., 2003). Lomb's analysis together with analysis of longer EEG records provided better resolution (0.5 Hz) than that obtained with FFT analysis (1.0 Hz). Although Lomb's and FFT analyses should provide very similar results (Manis et al., 2003), peak frequencies reported for the two analyses are not identical because Lomb's analysis used only a subset of the EEG records (continuous records of ≥ 3 s) that were used in the FFT analysis (records of ≥ 1 s).

Histology

After recording, each animal was perfused through the heart with 4% paraformaldehyde in 0.1 M phosphate buffer. After cryo-

protection with 30% sucrose in 0.1 M phosphate buffer, brains were sectioned on a freezing microtome. Sections through MSDB were prepared for immunohistochemical detection of parvalbumin (PV-ir) and choline acetyltransferase (ChAT-ir) as previously reported (Pang and Nocera, 1999). Sections containing PH, HPC, and PP were stained with Neutral Red or Cresyl Violet, and electrode locations were visualized with the Prussian Blue reaction. Based on qualitative visual inspection, rats were eliminated from data analysis if their stimulating/recording electrodes were placed in incorrect locations or their lesions were incomplete or nonselective. KA-treated rats were required to have complete or near-complete elimination of PV-ir neurons with minimal reduction of ChAT-ir neurons. Rats treated with SAP were required to have complete or near-complete loss of ChAT-ir neurons with minimal loss of PV-ir neurons.

Stereology

The effects of KA and SAP on MSDB ChAT- and PV-ir neurons were analyzed quantitatively using standard stereological procedures (West, 1999) by a person blind to the treatments. For the stereological analysis, saline-treated ($n = 3$), KA-treated ($n = 3$), and SAP-treated ($n = 3$) rats were randomly selected from the rats used in the data analysis. Every sixth section through the entire MSDB was counted, resulting in four to six total sections per cell type per animal. Stereological analysis was performed using the optical fractionator method (Stereo Investigator, MicroBrightField, Colchester, VT) and a microscope with an x-, y-, z-axis motorized stage (Bio Point 30, Ludl Electronic Products, Hawthorne, NY). Clearly identified ChAT-ir or PV-ir cell bodies were counted with a $63\times$ objective lens (Carl Zeiss, 1.4 NA). Cells in the uppermost focal plane ($3\mu\text{m}$) were not counted. The counting frame had an area of $8,500\mu\text{m}^2$ and a height of $15\mu\text{m}$.

RESULTS

Histology

Control rats showed dense PV-ir and ChAT-ir neuronal populations in MSDB (Fig. 1). Similar to our previous study (Pang et al., 2001), rats injected with KA had few or no PV-ir MSDB neurons with a large number of ChAT-ir neurons. KA treatment did not damage the CA3 region of HPC, as was observed in a subset of rats in a previous study (Pang et al., 2001) (Fig. 2). Rats injected with SAP had few or no ChAT-ir neurons in MSDB with many PV-ir neurons. Quantification of MSDB neurons using stereology supports these general findings (Fig. 3). Control rats had a mean (\pm SEM) of 6044 ± 482 PV-ir cells (range (R) = 5552–7008) and 6788 ± 298 ChAT-ir cells (R = 6348–7357). KA caused an 84% loss of PV-ir cells (987 ± 281 cells; R = 485–1265), but only an 8% loss of ChAT-ir cells (6239 ± 1009 cells; R = 4368–7827). In contrast, SAP produced an 89% loss of ChAT-ir cells (749 ± 336 cells; R = 323–1413), and only a 21% loss of PV-ir cells (4745 ± 996 cells; R = 3015–6464).

Recording During Urethane Anesthesia

No difference was seen between strains or sexes of rats in any of the recording conditions. Therefore, data from male Long-Evans and female Sprague-Dawley rats were combined for the analysis. Control rats showed some spontaneous synchronized activity within HPC θ bandwidth along with irregular activity. KA-treated and SAP-treated rats showed irregular activity with little or no obvious spontaneous HPC θ synchronization. However, some rats treated with KA or SAP demonstrated considerable amplitude variation at frequencies (2–3 Hz) below the HPC θ range during tail pinch or PH stimulation. The EEG records that showed increased amplitude of <4 Hz generally did

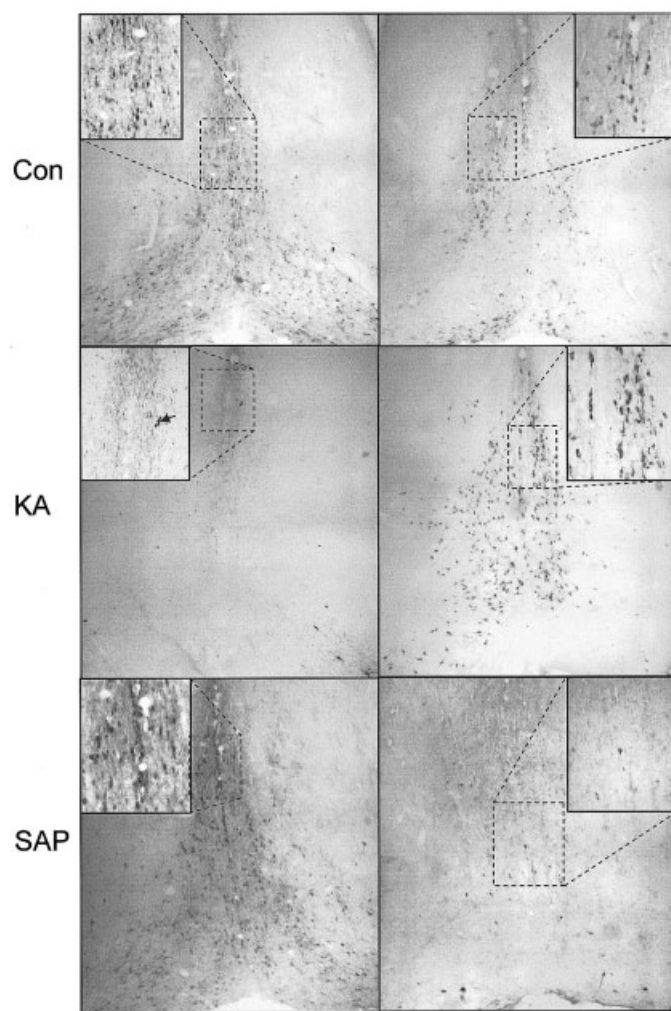


FIGURE 1. Sections of medial septum/diagonal band (MSDB) of Broca from control (Con), kainate-treated (KA), and 192 IgG-saporin-treated (SAP) rats. Left sections were stained for parvalbumin immunoreactivity (PV-ir) as a marker for γ -aminobutyric acid (GABA)ergic projection neurons. Right sections were stained for choline acetyltransferase immunoreactivity (ChAT-ir) as a marker for cholinergic neurons. Control rats had dense populations of PV-ir and ChAT-ir neurons. Kainate-treated rats showed ChAT-ir cells but few PV-ir cells, demonstrating loss of GABAergic neurons with little damage to cholinergic neurons. Arrow in inset points to damage caused during kainate injection. 192 IgG-saporin-treated rats showed PV-ir cells but few ChAT-ir cells, demonstrating loss of cholinergic neurons.

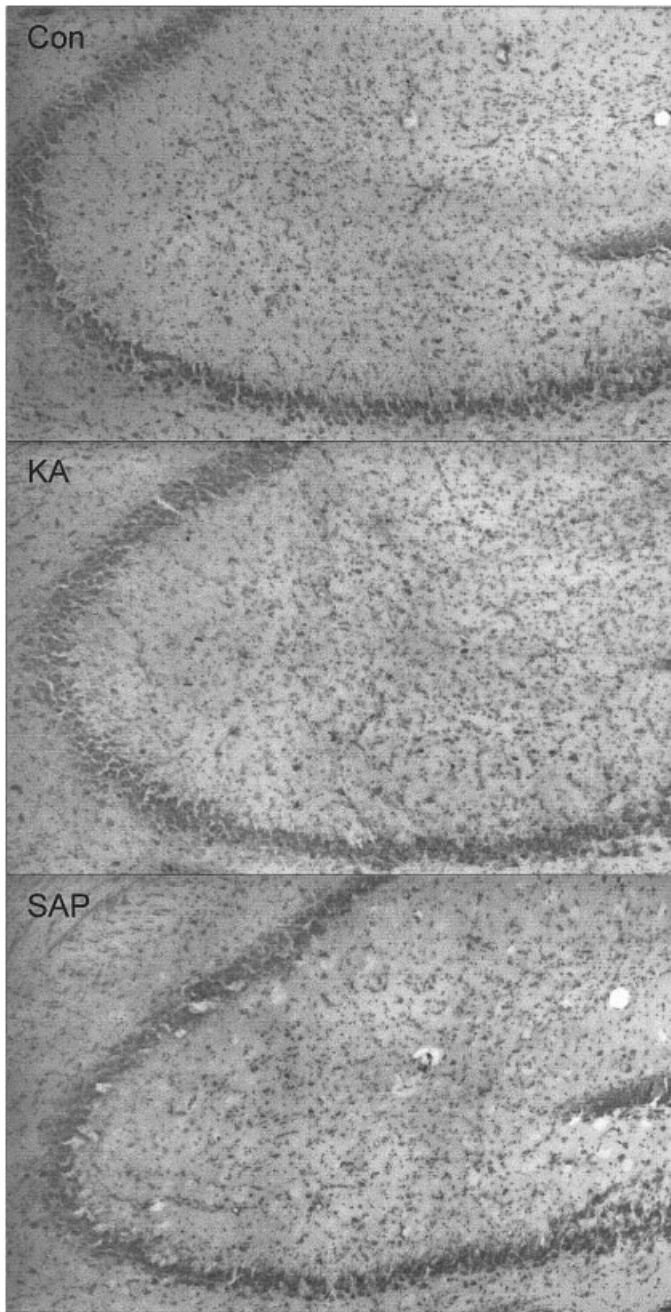


FIGURE 2. Representative coronal section through dorsal hippocampus area CA3. No damage to pyramidal cell layer was present after intraseptal injection of saline (Con), kainic acid (KA), or 192 IgG-saporin (SAP).

not have continuous activity at these frequencies throughout the 8-s EEG record. Therefore, the average amplitude value at 2–3 Hz may not be representative of the entire EEG sample. Although it is interesting that rats with KA or SAP lesions appeared to have a higher amplitude of low-frequency activity than that of control rats, this result was highly variable within each treatment group. Our peak frequency measure was determined from the greatest amplitude in the HPCθ range, even though the average amplitude of <4 Hz may be greater than the amplitude of 4–10 Hz.

Tail pinch

Septal KA and SAP lesions had a profound effect on tail pinch-induced HPCθ during urethane anesthesia (Figs. 4A and 5A). During tail pinch stimulation, EEG of control rats showed pronounced synchronized oscillation within HPCθ bandwidth. Control rats ($n = 7$) demonstrated a mean amplitude (\pm SEM) at peak frequency of $74.5 \pm 7.0 \mu\text{V}$ with a mean peak frequency of $5.3 \pm 0.2 \text{ Hz}$. In contrast, KA-treated and SAP-treated rats showed very little, if any, HPCθ activity during tail pinch stimulation. In most cases, a clear peak within 4–10 Hz was not observed for KA- and SAP-treated rats. However, to provide some quantification of the effects of these treatments, the frequency within 4–10 Hz with greatest amplitude was used as the peak frequency. For KA-treated rats ($n = 9$), the mean amplitude at peak frequency was $19.7 \pm 2.6 \mu\text{V}$, with a mean peak frequency of $5.8 \pm 0.4 \text{ Hz}$. SAP-treated rats ($n = 4$) had a mean amplitude of $22.5 \pm 3.6 \mu\text{V}$ with a mean peak frequency of $6.0 \pm 0.4 \text{ Hz}$. Treatment had a significant effect on amplitude at peak frequency, $F(2, 17) = 42.05$, $P < 0.0001$. Post hoc analysis revealed a significant reduction of HPCθ amplitude in KA versus control rats, $P < 0.0001$, and SAP versus control rats, $P < 0.0001$. HPCθ amplitude in KA- and SAP-treated rats was not significantly different, $P = 0.93$. Kainate or SAP did not alter peak frequency of HPCθ during tail pinch, $F(2, 17) = 0.78$, $P = 0.47$.

Integrated amplitude values at 12–15 Hz were $12.9 \pm 1.1 \mu\text{V}$ for control rats, $16.2 \pm 6.6 \mu\text{V}$ for KA-treated rats, and $9.7 \pm 1.2 \mu\text{V}$ for SAP-treated rats. KA and SAP treatment did not reliably alter amplitude at these frequencies outside the HPCθ range, $F(2, 17) = 0.335$, $P = 0.72$.

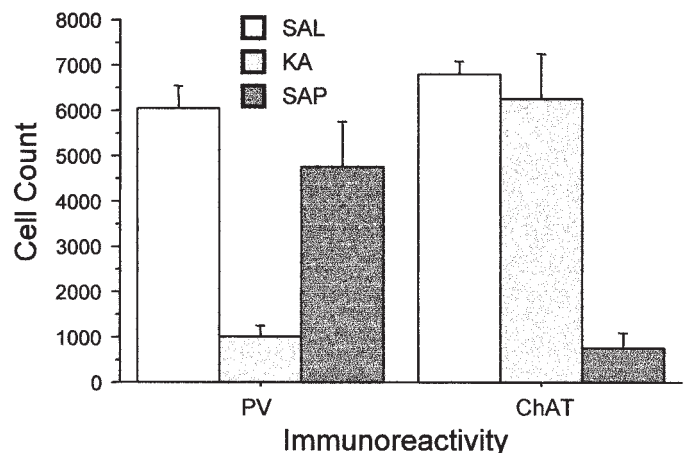


FIGURE 3. Mean \pm SEM number of parvalbumin (PV)- and choline acetyltransferase (ChAT)-ir cells remaining in medial septum/diagonal band (MSDB) after intraseptal injection of saline (SAL), kainate (KA), or 192 IgG-saporin (SAP). Compared with control rats, kainate-treated rats had an 83.7% reduction of PV-ir cells and an 8.1% reduction of ChAT-ir cells. Rats injected with 192 IgG-saporin had an 11.5% reduction of PV-ir and an 89.0% reduction of ChAT-ir cells.

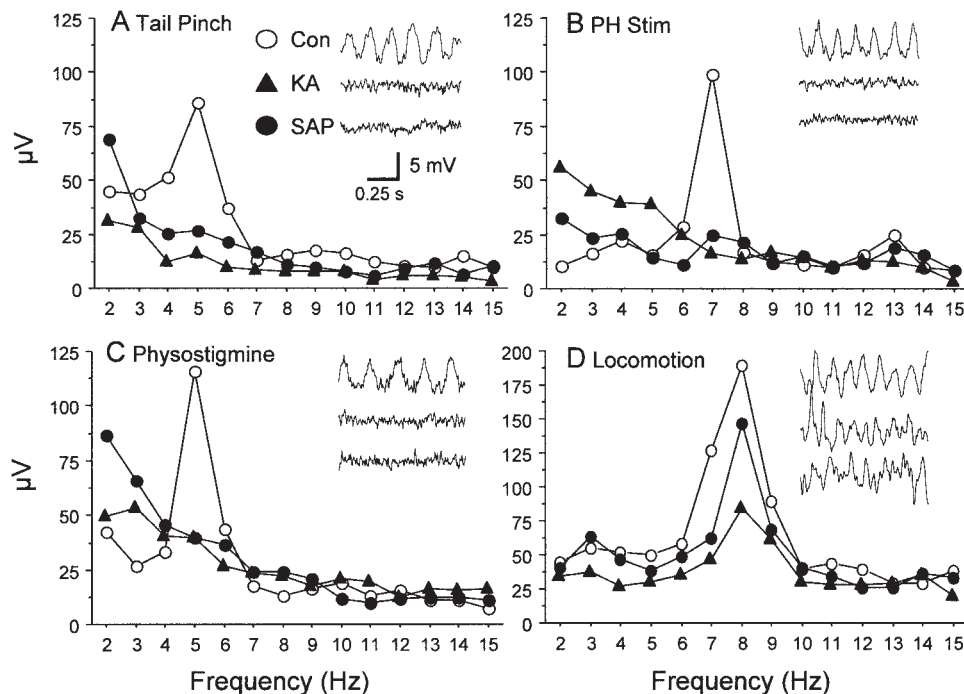


FIGURE 4. Fast Fourier Transform analyses from one representative animal per condition: control (Con), kainate (KA), and 192 IgG-saporin (SAP). Each FFT analysis is the average of 8 s; a 1-s EEG trace is included for each condition. **A:** Tail pinch stimulation during

urethane anesthesia. **B:** Posterior hypothalamus stimulation (400 μ A) during urethane anesthesia. **C:** 15-min post-injection of physostigmine during urethane anesthesia. **D:** Locomotion.

Posterior hypothalamus stimulation

Septal KA and SAP lesions dramatically reduced the HPC θ normally induced by 400- μ A PH stimulation during urethane anesthesia (Figs. 4B and 5A). During electrical PH stimulation, EEG of control rats ($n = 5$) showed pronounced oscillation within the HPC θ bandwidth, and FFT demonstrated a mean amplitude at a peak frequency of $117.0 \pm 16.5 \mu\text{V}$ with a mean peak frequency of $6.6 \pm 0.7 \text{ Hz}$. In contrast, KA-treated ($n = 9$) and SAP-treated ($n = 4$) rats showed very little, if any synchronous HPC θ activity during PH stimulation. Mean amplitude at peak frequency was $22.1 \pm 4.0 \mu\text{V}$ with a mean peak frequency of $6.7 \pm 0.5 \text{ Hz}$ for KA-treated rats. For SAP-treated rats, mean amplitude at peak frequency was $27.6 \pm 7.2 \mu\text{V}$ with a mean peak frequency of $6.3 \pm 0.5 \text{ Hz}$. Amplitude at peak frequency was different between treatments, $F(2, 15) = 32.794$, $P < 0.0001$. Post hoc analysis revealed significantly reduced amplitude in KA-treated versus control rats, $P < 0.0001$, and SAP-treated versus control rats, $P < 0.0001$. No difference was found between KA-treated and SAP-treated rats, $P = 0.92$. Treatments did not alter peak frequency of HPC θ induced by posterior hypothalamic stimulation, $F(2, 15) = 0.39$, $P = 0.68$.

The decreased HPC θ amplitude observed in KA-treated rats was paralleled by a reduction in amplitude of the EEG outside the HPC θ range, $F(2, 15) = 6.559$, $P = 0.009$. Integrated amplitude values from 12–15 Hz were $25.5 \pm 2.1 \mu\text{V}$ for control rats, $11.3 \pm 1.7 \mu\text{V}$ for KA-treated rats, and $16.7 \pm 6.0 \mu\text{V}$ for SAP-treated rats. Post hoc analysis revealed differences between control and KA

treatments ($P = 0.009$). All other comparisons were not significantly different ($P > 0.21$).

Systemic physostigmine

After systemic administration of physostigmine during urethane anesthesia, control rats ($n = 3$) showed continuous HPC θ after 5–10 min, whereas KA-treated ($n = 5$) and SAP-treated ($n = 4$) rats showed no HPC θ (Figs. 4C and 5A). In control rats, HPC θ activity continued to 30 min, at which time recording was terminated. The EEG records obtained at 15 min post-injection were used for comparison between control, KA-treated, and SAP-treated groups. Mean amplitude at peak frequency was $135.9 \pm 3.6 \mu\text{V}$ with a mean peak frequency of $5.3 \pm 0.7 \text{ Hz}$ for control rats, $15.9 \pm 1.8 \mu\text{V}$ with a mean peak frequency of $6.0 \pm 0.4 \text{ Hz}$ for KA-treated rats, and $26.5 \pm 4.6 \mu\text{V}$ with a mean peak frequency of $6.3 \pm 0.6 \text{ Hz}$ for SAP-treated rats. Amplitude at peak frequency was different between treatment groups, $F(2, 8) = 309.668$, $P < 0.0001$. Post hoc analysis showed that amplitude was reduced in rats with KA lesions versus controls, $P < 0.0001$, and SAP lesions versus controls, $P < 0.0001$. No difference was observed between KA-treated and SAP-treated rats, $P = 0.15$. Treatment did not alter the peak frequency of HPC θ , $F(2, 8) = 0.63$, $P = 0.56$.

The decreased HPC θ amplitude observed in KA-treated rats after systemic physostigmine injection was paralleled by a reduction in amplitude for frequencies outside the HPC θ range, $F(2, 8) = 4.434$, $P = 0.05$. Integrated amplitude values at 12–15 Hz were $15.2 \pm 1.4 \mu\text{V}$ for control rats, $8.8 \pm 0.8 \mu\text{V}$ for KA-treated

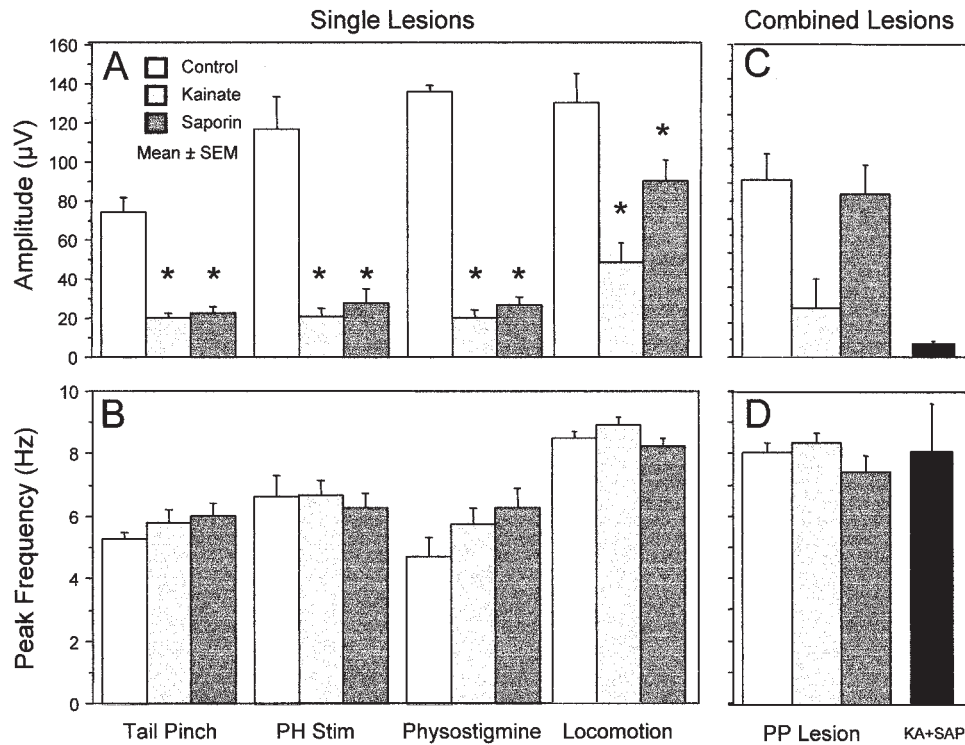


FIGURE 5. A: Single lesions of medial septum/diagonal band (MSDB). Amplitude (mean \pm SEM) HPC θ during urethane anesthesia with tail pinch, posterior hypothalamus (PH) stimulation, and systemic physostigmine, and during locomotion. B: Peak frequency during tail pinch, posterior hypothalamus stimulation, physostigmine, and locomotion. C: Combined lesions. Amplitude of HPC θ

during locomotion with combined MSDB and electrolytic perforant path lesion, and combined intraseptal γ -aminobutyric acid (GABA)ergic and cholinergic lesions induced by injection of kainate and 192 IgG-saporin. D: Peak frequency during locomotion with combined lesions. * $P < 0.05$

rats, and $11.5 \pm 1.9 \mu\text{V}$ for SAP-treated rats. Post hoc analysis revealed a difference between control and KA treatments ($P = 0.05$). All other comparisons were not significantly different ($P > 0.28$).

Depth profile

Peak amplitude of HPC θ is observed in CA1 and dentate gyrus (Bland and Whishaw, 1976). In an effort to assess whether intraseptal KA affects HPC θ in both of these regions, a depth profile was constructed from EEGs recorded between the dentate hilus and CA1 during tail pinch and PH stimulation. Depth of recording electrode was determined by the characteristic changes in the fEPSP evoked by electrical stimulation of the medial perforant path.

The recording electrode was positioned in the dentate hilus, 300 μm ventral to the dorsal blade of the granule cell layer. Location of the granule cell layer was determined by (1) reversal of the fEPSP, which occurs 100 μm dorsal to the dentate granule cell layer (Deadwyler et al., 1975); and (2) injury discharge of granule cells as the electrode passed through the cell layer. Depth of the perforant path stimulation electrode was adjusted to obtain maximum hilar population spike, indicating optimal stimulation of the medial PP. Recording began with the PP stimulating electrode optimally positioned. After records were obtained with tail pinch

and PH stimulation from each site, the recording electrode was raised in 100 μm steps from the dentate hilus through the CA1 pyramidal layer.

FFT analysis of EEG recorded from control rats ($n = 2$) revealed that maximum power of tail pinch-induced HPC θ occurred 100 μm dorsal to the dentate middle molecular layer, near the hippocampal fissure (Fig. 6A). In KA-treated rats ($n = 2$), no prominent HPC θ peaks were observed at any location in HPC or dentate gyrus during tail pinch. In control rats, PH stimulation (400 μA) showed maximum HPC θ amplitude 100 μm dorsal to the dentate middle molecular layer (Fig. 6B). Kainate-treated rats showed no HPC θ between the dentate hilus and CA1 during PH stimulation. These results suggest that lesions of GABAergic SH projections dramatically reduce HPC θ throughout the hippocampal formation in the urethane anesthetized rat.

Recordings During Locomotion

Single MSDB lesions

No difference was seen between strains or sexes of rats in any of the recording conditions. Therefore, data from male Long-Evans and female Sprague-Dawley rats were combined for all analyses. Locomotion-related HPC θ was attenuated, but not eliminated, after intraseptal KA or SAP treatment (Figs. 4D and 5A). FFT

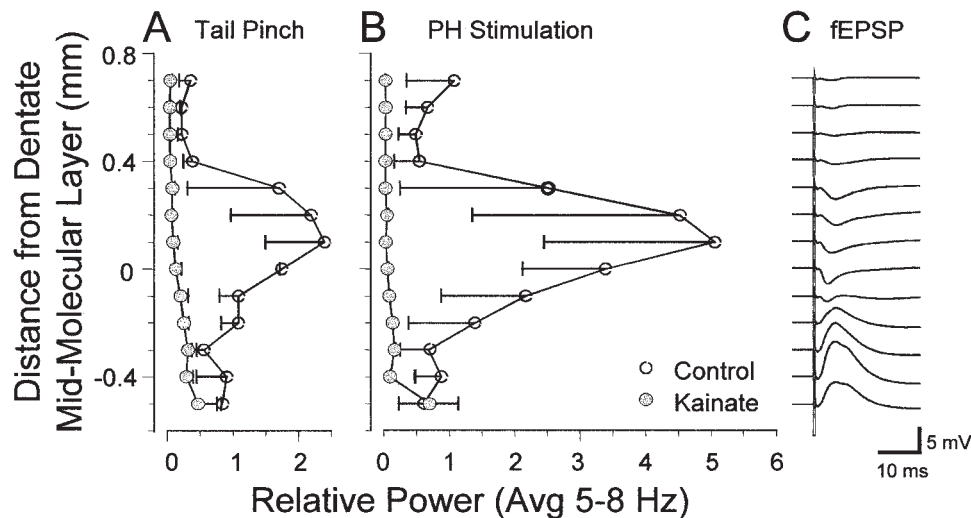


FIGURE 6. Depth profile of integrated HPCθ power from 5–8 Hz for urethane anesthetized saline- and kainate-treated rats during (A) tail pinch stimulation and (B) 400 μ A posterior hypothalamus stimulation. Representative field excitatory postsynaptic potential (C,

fEPSP) at each recording site in hippocampus with stimulating electrode in medial perforant path. fEPSP was used to estimate distance relative to middle molecular layer.

analysis of EEG recorded during spontaneous locomotion from control ($n = 7$) rats revealed a mean amplitude at peak frequency of $145.4 \pm 16.8 \mu\text{V}$ with a mean peak frequency of $8.4 \pm 0.2 \text{ Hz}$. Rats treated with KA ($n = 7$) and SAP ($n = 11$) showed reduced amplitude at peak frequency, although clear peaks were observed at $8.9 \pm 0.3 \text{ Hz}$ and $8.2 \pm 0.3 \text{ Hz}$ (mean peak frequency), respectively. Mean amplitude at peak frequency was $53.1 \pm 11.5 \mu\text{V}$ for KA-treated rats, and $99.9 \pm 12.3 \mu\text{V}$ for SAP-treated rats. ANOVA comparison between treatment groups demonstrated a significant alteration of HPCθ amplitude, $F(2, 22) = 9.681$, $P = 0.001$. Post hoc analysis revealed significantly reduced amplitude between control and KA rats, $P = 0.001$. The comparison between control and SAP treatments approached significance, $P = 0.08$, as did the KA and SAP comparison, $P = 0.07$. Medial septal treatments did not alter the mean peak frequency, $F(2, 22) = 1.76$, $P = 0.2$.

Integrated amplitude at 12–15 Hz during locomotion was $30.7 \pm 3.4 \mu\text{V}$ for control rats, $18.8 \pm 4.1 \mu\text{V}$ for KA-treated rats, and $26.2 \pm 2.4 \mu\text{V}$ for SAP-treated rats. Comparison of integrated amplitude (12–15 Hz) between control, KA-treated, and SAP-treated rats approached significance, $F(2, 22) = 3.041$, $P = 0.07$. The EEG recorded during alert immobility did not show any obvious differences between groups; large amplitude, irregular activity was present in control, KA-treated, and SAP-treated rats.

Combined MSDB and perforant path lesions

As described above, damage to either cholinergic or GABAergic septohippocampal neurons moderately reduced the amplitude of HPCθ during locomotion. To determine whether the EC is involved in the locomotion-related HPCθ resistant to selective MSDB lesions, bilateral PP lesions were made in control, KA-treated, and SAP-treated rats (Fig. 7). The amplitude of HPCθ before the PP lesion was compared with that recorded 1 day after

the PP lesion (Fig. 5C). For control rats ($n = 5$), HPCθ amplitude at peak frequency was $134.4 \pm 20.9 \mu\text{V}$ before PP lesion and $101.4 \pm 15.3 \mu\text{V}$ after PP lesion, resulting in an amplitude reduction of 24.6% by the PP lesion. Mean peak frequency was $8.4 \pm 0.3 \text{ Hz}$ before PP lesion and $8.0 \pm 0.3 \text{ Hz}$ after PP lesion. For KA-treated rats ($n = 3$), mean amplitude at peak frequency was $47.6 \pm 22.4 \mu\text{V}$ before the PP lesion and $27.7 \pm 16.0 \mu\text{V}$ after PP lesion, resulting in a 42.0% reduction of HPCθ amplitude by PP lesion. Mean peak frequency was $8.3 \pm 0.3 \text{ Hz}$ before PP lesion and $8.3 \pm 0.3 \text{ Hz}$ after PP lesion. For SAP-treated rats ($n = 5$), mean HPCθ amplitude at peak frequency was $103.7 \pm 15.6 \mu\text{V}$ before PP lesion and $92.9 \pm 16.3 \mu\text{V}$ after the lesion, resulting in a 10.4% amplitude reduction by PP lesion. Mean peak frequency

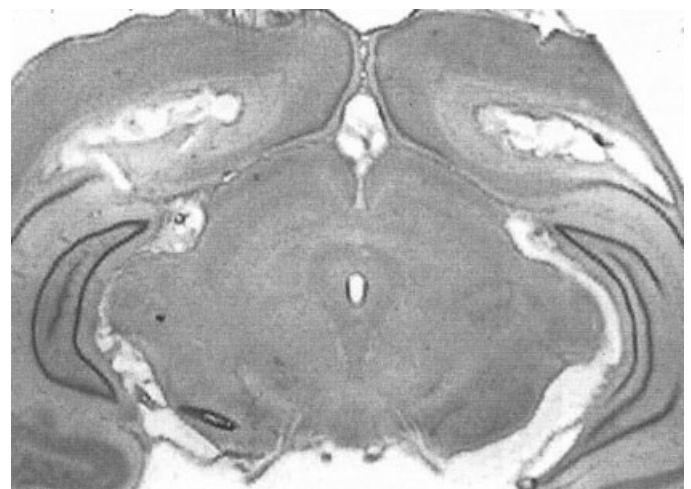


FIGURE 7. Coronal section through site of electrolytic perforant path lesion. Note: diagonal cut through cortex of left hemisphere was done post mortem.

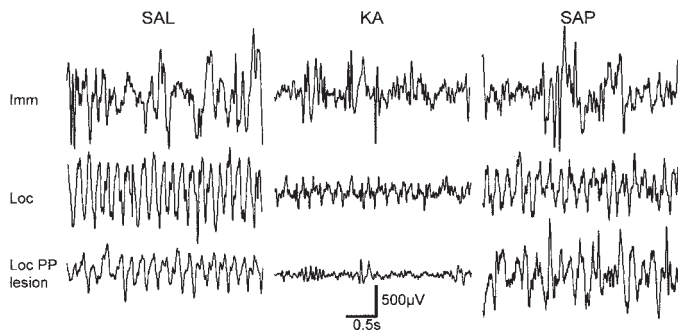


FIGURE 8. Example EEG traces recorded during alert immobility (Imm), locomotion (Loc), and locomotion after bilateral perforant path lesion (Loc PP Lesion) from one representative rat in each treatment group (SAL, intraseptal saline; KA, intraseptal kainic acid; SAP, intraseptal 192 IgG-saporin).

was 8.6 ± 0.02 Hz before PP lesion and 7.4 ± 0.5 Hz after PP lesion. Comparison of peak frequency after PP lesions showed there was no difference between treatment groups; $F(2, 10) = 1.16$, $P = 0.3522$. In summary, PP lesions reduced HPC θ amplitude in saline- and KA-injected rats, whereas the PP lesion produced very little additional reduction of HPC θ amplitude in SAP-treated rats (Fig. 8).

Combined MSDB KA + SAP lesions

Because previous studies demonstrated a loss of HPC θ after electrolytic lesions of the MSDB, fimbria/fornix transection, or nonselective MSDB lesions (Winson, 1978; M'Harzi and Monmaur, 1985; Gerashchenko et al., 2001), we were interested in the effects of combined KA and SAP lesions on HPC θ during locomotion. Two of the three rats that received combined intraseptal administration of KA and SAP had MSDB devoid of PV-ir and ChAT-ir neurons. For these two rats, mean amplitude at peak frequency was 10.8 ± 1.0 μ V with a mean peak frequency of 8.5 ± 1.5 Hz. Integrated amplitude outside the HPC θ frequency range was 8.6 ± 1.4 μ V. The third rat treated with KA and SAP had some sparing of ChAT-ir and PV-ir neurons, and data from this rat were therefore removed from the analysis. In general, rats treated with KA and SAP and with complete lesions of PV-ir and ChAT-ir neurons had a lower HPC θ amplitude than that of rats treated with either KA or SAP. Peak frequency did not appear to be altered by the combined KA and SAP lesion.

Lomb's analysis of peak frequency during locomotion

For further assessment of the effects of MSDB treatments on peak frequency, continuous EEG records of ≥ 3 s were subjected to a Lomb's analysis. Mean peak frequency (\pm SEM) using the Lomb's analysis was 10.0 ± 0.26 , 9.9 ± 0.38 , 9.3 ± 0.29 , 9.4 ± 1.15 Hz for saline, KA, SAP, and KA + SAP rats, respectively. As with the FFT analysis, none of the mean peak frequencies differed significantly between groups, $F(3,23) = 1.008$, $P = 0.4073$. Similar results were obtained from records obtained from rats with combined MSDB and PP lesions. Mean peak frequency was $9.4 \pm$

0.38 , 9.5 ± 0.96 , 10.8 ± 0.24 Hz for saline + PP, KA + PP, and SAP + PP rats, respectively. Like the FFT analysis, comparison of peak frequency during locomotion after combined MSDB and PP lesions showed no difference between groups, $F(2,10) = 1.966$, $P = 0.1906$. In summary, Lomb's analysis confirmed the lack of a shift in HPC θ peak frequency after MSDB lesions.

DISCUSSION

The present study examined the importance of GABAergic septohippocampal neurons for HPC θ during urethane anesthesia and locomotion. As a comparison, the effects of lesions of GABAergic septohippocampal neurons were compared with the effects of cholinergic septohippocampal lesions. MSDB GABAergic or cholinergic neurons were destroyed by intraseptal administration of KA or SAP, respectively. Hippocampal theta rhythm during urethane anesthesia was dramatically reduced after either intraseptal KA or SAP, suggesting that both GABAergic and cholinergic MSDB populations are necessary for type II HPC θ (HPC θ -2). During locomotion, HPC θ was moderately reduced in KA- or SAP-treated rats, suggesting that type I HPC θ remains despite the loss of either MSDB population. To further delineate the characteristics of the resistant HPC θ during locomotion, KA or SAP treatment was combined with PP lesions. The addition of a bilateral PP lesion to KA treatment virtually eliminated HPC θ during locomotion, whereas PP lesion combined with SAP treatment did not reduce HPC θ beyond that produced by either lesion alone. Furthermore, combined KA and SAP treatment, like the combination of PP lesion and KA treatment, reduced HPC θ beyond that observed with each lesion alone. Taken together, the results suggest that both GABAergic and cholinergic SH neurons are necessary for HPC θ -2. In addition, MSDB cholinergic and GABAergic, and EC glutamatergic projections are involved in HPC θ during locomotion.

In the present study, intraseptal injection of KA was used to destroy PV-ir neurons, while leaving most ChAT-ir neurons intact. PV-ir neurons in MSDB are GABAergic neurons (Freund, 1989), and ChAT-ir neurons are cholinergic neurons (Wainer et al., 1985). These two populations comprise the majority of the SH projection. In the basal forebrain, excitotoxins can have preferential actions on cholinergic or noncholinergic neurons depending on their selectivity to glutamate receptor subtypes (Dunnett et al., 1991). In the MSDB, injection of KA or ibotenic acid preferentially reduces glutamic acid decarboxylase (GAD) activity, and damages PV-ir and GAD-ir MSDB neurons, while having minimal effects on ChAT activity and the number of ChAT-ir neurons (Malthe-Sørensen et al., 1980; Walaas, 1981; Cahill and Baxter, 2001; Pang et al., 2001). In contrast, SAP administration to MSDB destroys cholinergic neurons, while leaving GABAergic neurons intact (Wiley et al., 1991). The present study quantified the effects of intraseptal KA and SAP using stereology, and the results agree with previous studies; that is, intraseptal KA preferentially destroys GABAergic septohippocampal cells, and intraseptal SAP selectively damages cholinergic septohippocampal neurons (Walaas, 1981; Berger-Sweeney et al., 1994; Heckers et al., 1994; Baxter et al., 1995; Pang et al., 2001). It must be noted, however,

that neurons other than PV-ir and ChAT-ir neurons exist in MSDB (Senut et al., 1989; Kiss et al., 1997), and some of these cells may be damaged by the neurotoxins. The present study did not assess the effects of KA or SAP on cells other than PV-ir and ChAT-ir neurons.

Intraseptal KA dramatically reduced HPC θ elicited by tail pinch or PH stimulation during urethane anesthesia. These results demonstrate the essential role of GABAergic septohippocampal neurons in HPC θ -2. Our results are the first demonstration that selective damage of GABAergic septohippocampal neurons eliminates HPC θ -2, and are consistent with current hypotheses suggesting that GABAergic MSDB neurons have a central role in HPC θ (Stewart and Fox, 1990; Lee et al., 1994; Wu et al., 2000). Septal GABAergic neurons rhythmically inhibit the inhibitory interneurons in HPC, effectively disinhibiting primary HPC cells and promoting HPC θ oscillations (Toth et al., 1997; Leung et al., 1994). Therefore, destruction of the GABAergic septohippocampal neurons appears to eliminate HPC θ by removing the rhythmic disinhibition of HPC pyramidal cells.

In contrast to the effects of intraseptal KA on HPC θ during urethane anesthesia, HPC θ during locomotion was moderately reduced, but not eliminated. The inability of KA to eliminate locomotion-related HPC θ suggests that MSDB GABAergic neurons play an important but not necessary role in locomotion-induced HPC θ . Reduction of HPC θ amplitude during locomotion may result from the elimination of HPC θ -2 without alteration of HPC θ -1, consistent with the idea that MSDB GABAergic neurons are involved only in HPC θ -2. This is supported by the observation that PP lesions attenuated the resistant HPC θ after intraseptal KA, similar to the finding that atropine combined with entorhinal cortex lesions abolishes locomotion-related HPC θ (Montoya and Sainsbury, 1985). However, elimination of HPC θ -2 with systemic atropine does not reduce locomotion HPC θ (Kramis et al., 1975), making our data more consistent with the possibility that intraseptal KA eliminates HPC θ -2 and reduces HPC θ -1. A reduction of HPC θ -1 (atropine-resistant) by MSDB GABAergic lesions would be consistent with the suggestion that GABAergic cells provide the atropine-resistant component of HPC θ (Stewart and Fox, 1990). Our results, however, demonstrate that MSDB GABAergic neurons cannot be solely responsible for HPC θ -1. Otherwise, intraseptal KA would have eliminated HPC θ during locomotion.

Like the effects of intraseptal KA, intraseptal SAP eliminated HPC θ -2 during urethane anesthesia, suggesting that cholinergic septohippocampal neurons are also necessary for HPC θ -2. Atropine, a muscarinic antagonist, eliminates HPC θ -2 during urethane anesthesia (Kramis et al., 1975; Monmaur et al., 1993). A common mechanism may underlie the effects of atropine and intraseptal SAP on HPC θ ; that is, both may prevent the action of acetylcholine in the hippocampus (Stewart and Fox, 1990). However, a recent study has demonstrated that atropine may also interfere with HPC θ by blockade of the cholinergic receptors on GABAergic septohippocampal neurons (Wu et al., 2000). Our results with intraseptal KA and SAP support both theories, providing evidence that both cholinergic and GABAergic MSDB neurons are necessary for HPC θ -2.

Similar to previous findings (Lee et al., 1994; Bassant et al., 1995), MSDB SAP lesions reduced the amplitude of, but did not eliminate, HPC θ during locomotion. As during urethane anesthesia, the effects of intraseptal SAP on locomotion-related HPC θ were similar to the effects of KA. A notable difference is that, whereas resistant HPC θ after KA is sensitive to PP lesion, the resistant HPC θ after SAP is not. In the present study, PP lesions did not further reduce the locomotion HPC θ remaining after intraseptal SAP lesions.

The effects of intraseptal KA or SAP depended on whether HPC θ was recorded during urethane anesthesia or during locomotion. What might account for these differences? Our studies suggest that EC input to hippocampus may be important for HPC θ during locomotion, and less so during urethane anesthesia. HPC θ involves the EC, which provides glutamatergic, excitatory projections to HPC (Vanderwolf and Leung, 1983; Montoya and Sainsbury, 1985; Vanderwolf et al., 1985a). Evidence for EC involvement in HPC θ generation is provided by a tight relation between θ -related activity in EC and HPC, which is eliminated in both locations by MSDB inactivation (Mitchell and Ranck, 1980; Dickson et al., 1995; Stewart et al., 1992; Jeffery et al., 1995). Furthermore, three times as many cells in medial EC are phase-locked to HPC θ during locomotion as are phase-locked during urethane anesthesia, suggesting that EC contributes more to HPC θ during locomotion than during urethane anesthesia (Stewart et al., 1992). Entorhinal cortical lesions alone reduce synchronized activity near the hippocampal fissure, but do not affect HPC θ activity at other regions of the dentate gyrus (Montoya and Sainsbury, 1985; Vanderwolf et al., 1985b; Partlo and Sainsbury, 1996). Hippocampal theta rhythm remaining after EC lesions can be eliminated by ACh antagonists, suggesting the EC lesions eliminate HPC θ -1 (atropine-insensitive) while HPC θ -2 (atropine-sensitive) remains (Vanderwolf and Leung, 1983; Montoya and Sainsbury, 1985). Concordant evidence is provided by the present investigation of MSDB GABAergic/EC contributions to locomotion HPC θ . In summary, elimination of locomotion-related HPC θ by the combination of MSDB GABAergic and PP lesions is consistent with the hypothesis that the EC provides the atropine resistant input to HPC, and MSDB GABAergic cells (which contain muscarinic receptors) provides the atropine-sensitive input to HPC.

Previous researchers have theorized that HPC θ requires a balance of excitatory and inhibitory influences in the hippocampus (Heynen and Bilkey; Stewart and Fox, 1990; Lee et al., 1994). This theory proposes that disturbing the balance of the excitatory (EC glutamatergic or MSDB cholinergic) and inhibitory (GABAergic septohippocampal neurons) inputs to the hippocampus would disrupt HPC θ . Our results with intraseptal injection of either KA or SAP support this idea for HPC θ -2, but the involvement of HPC afferents in locomotion HPC θ appears to be different. Results of our combined lesions suggest that excitatory and inhibitory inputs to the hippocampus may be responsible for separate components of locomotion-related HPC θ , and each HPC θ component can exist without the other, as demonstrated by MSDB KA or SAP lesions. Locomotion-related HPC θ is only eliminated by a combination lesion that destroys an excitatory (EC glutamatergic or MSDB cholinergic) and an inhibitory (MSDB GABAergic) input to hippocampus. It is noteworthy that damage to both excitatory

inputs did not result in a further attenuation of HPC θ than each individual lesion. Although the excitatory actions of glutamate and ACh on hippocampal neurons differ from each other (Cole and Nicoll, 1984), our results suggest these two excitatory HPC afferents may be functionally redundant with regard to locomotion-related HPC θ .

In addition to the cholinergic SH projection, it is possible that the septo-entorhinal cholinergic projection is involved in HPC θ -1. The ACh projection from MSDB to EC may facilitate the EC theta activity (Mitchell et al., 1982; Jeffery et al., 1995). Removal of the PP would not be expected to reduce HPC θ amplitude further than MSDB cholinergic lesions alone if the primary action of MSDB cholinergic neurons on locomotion HPC θ is through the EC. Alternatively, the EC may play only a minor role in locomotion HPC θ synchronization, and theta activity in EC may be synchronized by the same mechanism (i.e., the MSDB neurons) as in HPC. Thus, the results of the present study suggest MSDB cholinergic and GABAergic neurons interact differently in urethane-related HPC θ and locomotion-related HPC θ .

Functional Significance

It has been suggested that HPC θ is required for spatial learning and memory (see review by Vertes and Kocsis, 1997). Long-term potentiation is preferentially induced with HPC θ -frequency bursts and on HPC θ peaks (Larson et al., 1986; Rose and Dunwiddie, 1986; Diamond et al., 1988; Pavlides et al., 1988; Holscher et al., 1997; Hyman et al., 2003), suggesting HPC θ is a mechanism by which HPC forms associations between stimuli. Nonspecific MSDB lesions or inactivation with tetracaine eliminates HPC θ , and causes performance deficits on spatial and nonspatial memory tasks (Winson, 1978; Givens and Olton, 1990; Mizumori et al., 1990). Lack of spatial memory deficits after KA or SAP lesions of medial septum (Baxter et al., 1995; McMahon et al., 1997; Pang et al., 2001) may be at least partially explained by the continued, albeit reduced, presence of locomotion-related HPC θ after these lesions.

SUMMARY

The present study demonstrates that MSDB GABAergic or MSDB cholinergic lesions block HPC θ during urethane anesthesia, whereas either lesion alone reduces, but does not eliminate, HPC θ during locomotion. When combined with EC disconnection, MSDB GABAergic lesions, but not MSDB cholinergic lesions, virtually eliminate HPC θ during locomotion. Combined MSDB GABAergic and cholinergic lesions also appear to eliminate HPC θ during locomotion. Based on our data and those from previous studies, we propose the following summary to describe the interaction between MSDB and EC in HPC θ . Septal GABAergic cells inhibit HPC interneurons whereas MSDB cholinergic and EC glutamatergic cells directly excite HPC cells, although the time course of the effects of acetylcholine and glutamate are markedly different. Locomotion-related HPC θ involves an inhibitory input from MSDB and an excitatory input to HPC, which can come from MSDB or EC. In contrast, HPC θ under urethane anesthesia

requires both the inhibitory and excitatory MSDB inputs to HPC, possibly because of the reduced EC input under anesthesia. The present results support the hypothesis that a balance between inhibitory and excitatory HPC inputs is necessary for HPC θ (Stewart and Fox, 1990; Heynen and Bilkey, 1991).

Acknowledgments

The authors thank Jaak Panksepp, Verner Bingman, and J. Devin McAuley for comments.

REFERENCES

- Bassant MH, Apartis E, Jazat-Poindessous FR, Wiley RG, Lamour YA. 1995. Selective immunolesion of the basal forebrain cholinergic neurons: effects on hippocampal activity during sleep and wakefulness in the rat. *Neurodegeneration* 4:61–70.
- Baxter MG, Bucci DJ, Gorman LK, Wiley RG, Gallagher M. 1995. Selective immunotoxic lesions of basal forebrain cholinergic cells: effects on learning and memory in rats. *Behav Neurosci* 109:714–722.
- Berger-Sweeney J, Heckers S, Mesulam MM, Wiley RG, Lappi DA, Sharma M. 1994. Differential effects on spatial navigation of immunotoxin-induced cholinergic lesions of the medial septal area and nucleus basalis magnocellularis. *J Neurosci* 14:4507–4519.
- Bland BH, Whishaw IQ. 1976. Generators and topography of hippocampal theta (RSA) in the anesthetized and freely moving rat. *Brain Res* 118:259–280.
- Brazhnik ES, Fox SE. 1997. Intracellular recordings from medial septal neurons during hippocampal theta rhythm. *Exp Brain Res* 114:442–453.
- Cahill JF, Baxter MG. 2001. Cholinergic and noncholinergic septal neurons modulate strategy selection in spatial learning. *Eur J Neurosci* 14:1856–1864.
- Cole AE, Nicoll RA. 1984. Characterization of a slow cholinergic postsynaptic potential recorded in vitro from rat hippocampal pyramidal cells. *J Physiol* 352:173–188.
- Deadwyler SA, West JR, Cotman CW, Lynch GS. 1975. A neurophysiological analysis of commissural projections to dentate gyrus of the rat. *J Neurophysiol* 38:167–184.
- Diamond DM, Dunwiddie TV, Rose GM. 1988. Characteristics of hippocampal primed burst potentiation in vitro and in the awake rat. *J Neurosci* 8:4079–4088.
- Dickson CT, Kirk IJ, Oddie SD, Bland BH. 1995. Classification of theta-related cells in the entorhinal cortex: cell discharges are controlled by the ascending brainstem synchronizing pathway in parallel with hippocampal theta-related cells. *Hippocampus* 5:306–319.
- Dunnett SB, Everitt BJ, Robbins TW. 1991. The basal forebrain-cortical cholinergic system: interpreting the functional consequences of excitotoxic lesions. *Trends Neurosci* 14:494–501.
- Freund TF. 1989. GABAergic septohippocampal neurons contain parvalbumin. *Brain Res* 478:375–381.
- Gerashchenko D, Salin-Pascual R, Shiromani PJ. 2001. Effects of hypocretin-saporin injections into the medial septum on sleep and hippocampal theta. *Brain Res* 913:106–115.
- Givens BS, Olton DS. 1990. Cholinergic and GABAergic modulation of medial septal area: effect on working memory. *Behav Neurosci* 6:849–855.
- Green JD, Arduini AA. 1954. Hippocampal electrical activity in arousal. *J Neurophysiol* 17:533–557.
- Heckers S, Ohtake T, Wiley RG, Lappi DA, Geula G, Mesulam MM. 1994. Complete and selective cholinergic denervation of rat neocortex and hippocampus but not amygdala by an immunotoxin against the p75 NGF receptor. *J Neurosci* 14:1271–1289.

- Heynen AJ, Bilkey DK. 1991. Induction of RSA-like oscillations in both the in-vitro and in-vivo hippocampus. *NeuroReport* 2:401–404.
- Holscher C, Anwyl R, Rowan MJ. 1997. Stimulation on the positive phase of hippocampal theta rhythm induces long-term potentiation that can be depotentiated by stimulation on the negative phase in area CA1 in vivo. *J Neurosci* 17:6470–6477.
- Hyman, JM, Wyble BP, Goyal V, Rossi CA, Hasselmo ME. 2003. Stimulation in hippocampal region CA1 in behaving rats yields long-term potentiation when delivered to the peak of theta and long-term depression when delivered to the trough. *J Neurosci* 23:11725–11731.
- Jeffery KJ, Donnett JG, O'Keefe J. 1995. Medial septal control of theta-correlated unit firing in the entorhinal cortex of awake rats. *NeuroReport* 6:2166–2170.
- Kiss J, Magloczy Z, Somogyi J, Freund TF. 1997. Distribution of calretinin-containing neurons relative to other neurochemically identified cell types in the medial septum of the rat. *Neuroscience* 78:399–410.
- Kramis R, Vanderwolf CH, Bland BH. 1975. Two types of hippocampal rhythmical slow activity in both the rabbit and the rat: relations to behavior and effects of atropine, diethyl ether, urethane, and pentobarbital. *Exp Neurol* 49:58–85.
- Larson J, Wong D, Lynch G. 1986. Patterned stimulation at theta frequency is optimal for the induction of long-term potentiation. *Brain Res* 368:347–350.
- Lawson VH, Bland BH. 1993. The role of the septohippocampal pathway in the regulation of hippocampal field activity and behavior: analysis by the intraseptal microinfusion of carbachol, atropine, and procaine. *Exp Neurol* 120:132–144.
- Lee MG, Chrobak JJ, Sik A, Wiley RG, Buszaki G. 1994. Hippocampal theta activity following selective lesion of the septal cholinergic system. *Neuroscience* 62:1033–1047.
- Leung LS, Martin L-A, Stewart DJ. 1994. Hippocampal theta rhythm in behaving rats following ibotenic acid lesion of the septum. *Hippocampus* 4:136–147.
- Malthe-Sørensen D, Odden E, Walaas I. 1980. Selective destruction by kainic acid of neurons innervated by putative glutamatergic afferents in septum and nucleus of the diagonal band. *Brain Res* 182:461–465.
- Manis PB, Molitor SC, Wu H. 2003. Subthreshold oscillations generated by TTX-sensitive sodium currents in dorsal cochlear nucleus pyramidal cells. *Exp Brain Res* 153:443–451.
- McMahon RW, Sobel TJ, Baxter MG. 1997. Selective immunolesions of hippocampal cholinergic input fail to impair spatial working memory. *Hippocampus* 7:130–136.
- M'Harzi M, Monmaur P. 1985. Selective lesions of the fimbria and the fornix in the rat: differential effects on CA1 and dentate theta. *Exp Neurol* 89:361–371.
- Mitchell SJ, Rawlins JN, Steward O, Olton DS. 1982. Medial septal area lesions disrupt theta rhythm and cholinergic staining in medial entorhinal cortex and produce impaired radial arm maze behavior in rats. *J Neurosci* 2:292–302.
- Mitchell SJ, Ranck JB. 1980. Generation of theta rhythm in medial entorhinal cortex of freely moving rats. *Brain Res* 189:49–66.
- Mizumori SJY, Barnes CA, McNaughton BL. 1989. Reversible inactivation of the medial septum: selective effects on the spontaneous unit activity of different hippocampal cell types. *Brain Res* 500:99–106.
- Mizumori SJY, Perez GM, Alvarado MC, Barnes CA, McNaughton BL. 1990. Reversible inactivation of the medial septum differentially affects two forms of learning in rats. *Brain Res* 528:12–20.
- Monmaur P, Breton P. 1990. Elicitation of hippocampal theta by intraseptal carbachol injection in freely moving rats. *Brain Res* 544:150–155.
- Monmaur P, Ayadi K, Breton P. 1993. Hippocampal EEG responses induced by carbachol and atropine infusions into the septum and the hippocampus in the urethane-anesthetized rat. *Brain Res* 631:317–324.
- Montoya CP, Sainsbury RS. 1985. The effects of entorhinal cortex lesions on Type 1 and Type 2 theta. *Physiol Behav* 35:121–126.
- Oddie SD, Stefanek W, Kirk IJ, Bland BH. 1996. Intraseptal procaine abolishes hypothalamic stimulation-induced wheel-running and hippocampal theta field activity in rats. *J Neurosci* 16:1948–1956.
- Pang KCH, Nocera R. 1999. Interactions between 192 IgG-saporin and intraseptal cholinergic and GABAergic drugs: role of cholinergic medial septal neurons in spatial working memory. *Behav Neurosci* 113:265–275.
- Pang KCH, Nocera R, Secor AJ, Yoder RM. 2001. GABAergic septohippocampal neurons are not necessary for spatial memory. *Hippocampus* 11:814–827.
- Partlo LA, Sainsbury RS. 1996. Influence of medial septal and entorhinal cortex lesions on theta activity recorded from the hippocampus and median raphe nucleus. *Physiol Behav* 59:887–895.
- Pavlidis C, Greenstein YJ, Grudman M, Winson J. 1988. Long-term potentiation in the dentate gyrus is induced preferentially on the positive phase of theta rhythms. *Brain Res* 439:383–387.
- Rose GM, Dunwiddie TV. 1986. Induction of hippocampal long-term potentiation using physiologically patterned stimulation. *Neurosci Lett* 69:244–248.
- Senut MC, Menetrey D, Lamour Y. 1989. Cholinergic and peptidergic projections from the medial septum and the nucleus of the diagonal band of Broca to dorsal hippocampus, cingulate cortex and olfactory bulb: a combined wheatgerm agglutinin-aphorseradish peroxidase-gold immunohistochemical study. *Neuroscience* 30:385–403.
- Stewart M, Fox SE. 1990. Do septal neurons pace the hippocampal theta rhythm? *Trends Neurosci* 13:163–168.
- Stewart M, Quirk GJ, Barry M, Fox SE. 1992. Firing relations of medial entorhinal neurons to the hippocampal theta rhythm in urethane anesthetized and walking rats. *Exp Brain Res* 90:21–28.
- Toth K, Freund TF, Miles R. 1997. Disinhibition of rat hippocampal pyramidal cells by GABAergic afferents from the septum. *J Physiol* 500:463–474.
- Vanderwolf CH. 1969. Hippocampal electrical activity and voluntary movement in the rat. *Electroencephalogr Clin Neurophysiol* 26:407–418.
- Vanderwolf CH. 1975. Neocortical and hippocampal activation in relation to behavior: effects of atropine, eserine, phenothiazines, and amphetamine. *J Comp Physiol Psychol* 88:300–323.
- Vanderwolf CH, Leung L-WS. 1983. Hippocampal rhythmical slow activity: a brief history and the effects of entorhinal lesions and phencyclidine. In: Seifert W, editor. *Neurobiology of the hippocampus*. London: Academic Press. p 275–302.
- Vanderwolf CH, Leung, LWS, Cooley RK. 1985a. Pathways through cingulate, neo- and entorhinal cortices mediate atropine-resistant hippocampal rhythmical slow activity. *Brain Res* 347:58–73.
- Vanderwolf CH, Leung L-WS, Stewart DJ. 1985b. Two afferent pathways mediating hippocampal rhythmical slow activity. In: Buzsaki G, Vanderwolf CH, editors. *Electrical activity of the archicortex*. Budapest: Akadémiai Kiadó. p 47–66.
- Vertes RP, Kocsis B. 1997. Brainstem-diencephalo-septohippocampal systems controlling the theta rhythm of the hippocampus. *Neuroscience* 81:893–926.
- Wainer BH, Levey AI, Rye DB, Mesulam MM, Mufson EJ. 1985. Cholinergic and non-cholinergic septohippocampal pathways. *Neurosci Lett* 54:45–52.
- Walaas I. 1981. The effects of kainic acid injections on guanylate cyclase activity in the rat caudatoputamen, nucleus accumbens and septum. *J Neurochem* 36:233–241.
- West MJ. 1999. Stereological methods for estimating the total number of neurons and synapses: issues of precision and bias. *Trends Neurosci* 22:2:51–61.
- Wiley RG, Oeltmann TN, Lappi DA. 1991. Immunolesioning: selective destruction of neurons using immunotoxin to rat NGF receptor. *Brain Res* 562:149–153.
- Winson J. 1978. Loss of hippocampal theta rhythm results in spatial memory deficit in the rat. *Science* 201:160–163.
- Wu M, Shanabrough M, Leranath C, Alreja M. 2000. Cholinergic excitation of septohippocampal GABA but not cholinergic neurons: implications for learning and memory. *J Neurosci* 20:3900–3908.